JP2.12 AN ANALYTIC MODEL OF THE VERTICAL CARBON DIOXIDE RECTIFIER EFFECT

Vincent E. Larson[1]*, Hans Volkmer[1]
[1] Dept. of Mathematical Sciences, University of Wisconsin — Milwaukee, Milwaukee, WI

1. INTRODUCTION: WHAT IS THE RECTIFIER EFFECT?

The flux of carbon dioxide (CO_2) from the land surface to the atmosphere undergoes a diurnal cycle. During the day, photosynthesis occurs, leading to a net flux of CO_2 from the atmosphere to biomass. During the night, respiration of CO_2 to the atmosphere occurs because of, e.g., plant decomposition. This oscillating diurnal flux of CO_2 is more or less symmetric between day and night, and is roughly sinusoidal (Baker et al. 2003; Davis et al. 2003).

In contrast to the *flux*, the near-surface time series of CO_2 *mixing ratio* is often asymmetric. In particular, the mixing ratio often peaks sharply in the wee hours of the morning and exhibits a long period of moderately low values during the day. Rather than being symmetric, the near-surface mixing ratio time series has a truncated sinusoidal appearance reminiscent of a rectified electrical alternating current (Heimann et al. 1986; Keeling et al. 1989; Denning et al. 1995, 1996a,b, 1999; Yi et al. 2000).

Given the quasi-symmetry of the time series of CO_2 *flux*, the observed asymmetry of the time series of *mixing ratio* may at first seem paradoxical. This diurnal rectifier effect results from differences in turbulent mixing between night and day (Denning et al. 1996b). During the night, the atmospheric boundary layer is often stable and shallow, causing CO_2 mixing ratio to build up strongly in a thin layer near the surface. During the day, the boundary layer is often convective and deep, causing the deficit in mixing ratio to be diluted over a large vertical extent. The resulting time-average vertical profile of CO_2 has an excess of CO_2 near the ground and a deficit aloft.

The rectifier effect is important in part because of its effect on inverse model calculations. Inverse models typically use measurements of CO_2 *mixing ratio* near the land or ocean surface and infer CO_2 *flux* at the surface. The surface flux, in turn, tells us about sources or sinks of CO_2 within the biosphere or ocean. In contrast to the highly localized fluxes yielded by direct measurement, inverse modeling yields average surface fluxes over broad areas, which is sometimes desirable. In the past, inverse modeling has been used primarily to derive CO_2 fluxes over continental-scale areas and monthly time scales, given near-surface observations of CO_2 mixing ratio at locations far from land (e.g. Gurney et al. 2002, 2003). However, there has also been interest in inverse calculations over land at sub-continental scales (Peylin et al. 2005; Bakwin et al. 2004) and diurnal or sub-diurnal timescales (e.g. Law et al. 2004; Braswell et al. 2005).

The rectifier effect influences inverse calculations in part because it increases the time-averaged CO_2 mixing ratio near the surface. If this increase is not taken into account in a forward model, it may lead to an overestimate of a CO_2 source or an underestimate of a sink (Denning et al. 1995, 1996a; Gurney et al. 2002, 2003; Stephens et al. 2007).

The one-dimensional rectifier effect has been observed and numerically simulated in prior works (e.g. Chen et al. 2004; Yi et al. 2004). The present paper develops an analytic, 1D, eddy-diffusivity model of it. Our primary goal is better conceptual understanding of the physics of the rectifier effect. However, the model may also be useful for inexpensive, approximate calculations, particularly analyses of tall-tower measurements of CO_2 mixing ratio that are used to invert diurnally varying sources and sinks at the surface. Inverse calculations may be facilitated by the fact that our model solutions depend only on a single non-dimensional parameter. Forward calculations may benefit from the fact that this single parameter can be used to prescribe the strength of the rectifier effect.

The structure of this paper is as follows. The model equation and boundary conditions are introduced in Section 2. Derivations of when these equations yield rectified solutions are presented in Sections 3 and 4. An analytic series solution is presented and plotted in Section 5. An application to inverse modelling is illustrated in Section 6. Conclusions are listed in Section 7.

2. MODEL SET-UP

The geometry of the problem is assumed to be a horizontally uniform layer extending from the ground up to an infinite altitude. Therefore the problem is spatially 1D in the vertical coordinate. We will use a tilde to denote variables having units and use no tilde for dimensionless variables. In contrast, for *constants or parameters*, no tilde will be used, regardless of whether they are dimensional or dimensionless.

We assume that turbulent transport is adequately modeled by an eddy diffusivity, $\tilde{K}$. Therefore, the atmospheric evolution of CO_2 is described by a diffusion

*Corresponding author address: Vincent E. Larson, Department of Mathematical Sciences, University of Wisconsin – Milwaukee, P. O. Box 413, Milwaukee, WI 53201-0413, vlarson at uwm dot edu, http://www.uwm.edu/∼vlarson .

equation for CO_2 mixing ratio. We will work in the *perturbation* mixing ratio, $\tilde{c}(\tilde{z},\tilde{t})$, from a reference value, $\tilde{c}_{\rm ref}$. We choose $\tilde{c}_{\rm ref}$ to equal the average of $\tilde{c}(\tilde{z},\tilde{t})$ over time $\tilde{t}$ *and* altitude $\tilde{z}$ that would occur if there were no source. The diffusion equation is:

$$\frac{\partial\tilde{c}(\tilde{z},\tilde{t})}{\partial\tilde{t}} = \frac{\partial}{\partial\tilde{z}}\left(\tilde{K}(\tilde{z},\tilde{t})\frac{\partial\tilde{c}(\tilde{z},\tilde{t})}{\partial\tilde{z}}\right) + \tilde{S}(\tilde{t}). \qquad (1)$$

Here $\tilde{S}$ is an internal atmospheric source of CO_2 that we allow to vary in time but not in the vertical direction. Although CO_2 does not have a significant chemical source in the atmosphere, $\tilde{S}$ may crudely represent specified, column-averaged horizontal advection of CO_2.

At the lower boundary ($\tilde{z}=0$) we impose a diurnal, sinusoidal flux of carbon because observed fluxes are often quasi-sinusoidal (e.g. Baker et al. 2003):

$$-\tilde{K}\frac{\partial\tilde{c}}{\partial\tilde{z}}\bigg|_{\tilde{z}=0} = F_0\cos(\omega_0\tilde{t}). \qquad (2)$$

Here $\omega_0 = 2\pi/(24\ \text{hours})$ is the angular frequency corresponding to one day, and F_0 is the maximum surface flux, with units of mixing ratio times velocity. We interpret $\tilde{t}=0$ as midnight local time.

At the upper boundary ($\tilde{z}\to\infty$), we impose a CO_2 flux of zero:

$$-\tilde{K}(\tilde{z},\tilde{t})\frac{\partial\tilde{c}(\tilde{z},\tilde{t})}{\partial\tilde{z}}\bigg|_{\tilde{z}=\infty} = 0. \qquad (3)$$

We place the upper boundary at infinity in order to simplify the analytic solutions. However, the main variation in CO_2 occurs near the lower boundary, specifically, within the atmospheric boundary layer, which over land tends to be shallow at night [O($\sim$ 100m)] and deeper during the day [O($\sim$ 1 km)] (e.g., Fig. 1.7 of Stull 1988; Yi et al. 2001).

We do not attempt to solve an initial value problem. Therefore we do not impose any initial condition. Instead, we assume periodic forcing and seek periodic solutions in time.

Now we non-dimensionalize the diffusion equation and boundary conditions. We choose a diffusivity scale $K_0 \approx 100$ to 1000 m^2 s^{-1}, a length scale $H = (2K_0/\omega_0)^{1/2} \approx 2$ to 5 km, a time scale $1/\omega_0$ equal to radians per day, and a CO_2 mixing ratio of

$$c_0 = F_0/(2\omega_0 K_0)^{1/2}. \qquad (4)$$

Then the equation and boundary conditions become

$$\frac{\partial c(z,t)}{\partial t} = \frac{\partial}{\partial z}\left(\frac{K(z,t)}{2}\frac{\partial c(z,t)}{\partial z}\right) + S(t), \qquad (5)$$

$$-\frac{K(z,t)}{2}\frac{\partial c(z,t)}{\partial z}\bigg|_{z=0} = \cos(t), \qquad (6)$$

and

$$-\frac{K(z,t)}{2}\frac{\partial c(z,t)}{\partial z}\bigg|_{z=\infty} = 0, \qquad (7)$$

where

$$c = (\tilde{c}-\tilde{c}_{\rm ref})/c_0, \qquad (8)$$

and $K=\tilde{K}/K_0$, $t=\omega_0\tilde{t}$, $z=\tilde{z}/H$, and $S=\tilde{S}/(\omega_0 c_0)$. The choice of length scale introduces factors of 2 into the equation and boundary conditions but simplifies the solutions below.

3. WHEN IS THE TIME-AVERAGED PROFILE OF CO_2 UNIFORM WITH ALTITUDE?

Prior works have noted that the rectifier effect stems from a non-zero temporal correlation between the surface flux of CO_2 and atmospheric vertical transport (Heimann et al. 1986; Keeling et al. 1989; Denning et al. 1996b; Stephens et al. 2000). Although we have not found a proof of this relationship, we now prove a somewhat related link between the concentration/transport covariance and the shape of the time-average CO_2 profile. In this section, we assume that the solution is time-periodic and that the time-averaged internal source of CO_2 vanishes, that is, that $\overline{S}^t = 0$.

We investigate the conditions under which the time average of CO_2 is uniform in the vertical, which corresponds to $\overline{c(z,t)}^t = 0$ at all altitudes. That is, we ask, When is

$$\overline{c(z,t)}^t \equiv \frac{1}{2\pi}\int_{-\pi}^{\pi} c(z,t)dt = 0? \qquad (9)$$

Such a uniform profile is associated with an un-rectified solution.

Larson and Volkmer (2008) show that

$$\overline{K\frac{\partial c}{\partial z}}^t = \text{Constant} = 0 \qquad (10)$$

at all altitudes, where we conclude that $\text{Constant} = 0$ because the upper boundary condition (7) imposes zero flux at the top boundary. The result (10) depends only on the assumptions of 1D transport (5), periodicity, zero source $S(t)$, and zero flux at the upper boundary (7). The result holds true for both rectified and unrectified cases.

If we distinguish the two cases, however, we can go further. If the diurnally averaged flux is zero (Eq. 10), then the daytime flux must be equal in magnitude but opposite in sign to the nighttime flux:

$$\overline{K\frac{\partial c}{\partial z}}^{\rm Day} = -\overline{K\frac{\partial c}{\partial z}}^{\rm Night}. \qquad (11)$$

If the transport, here modeled by $K(>0)$, is greater during the day than during the night, then $\partial c/\partial z$ must be smaller in magnitude during day than during night, which suggests a non-uniform (rectified) profile. Larson and Volkmer (2008) provide a formal proof. A rectified profile, in turn, corresponds to $\overline{c(z,t)}^t \neq 0$.

4. WHEN IS THE TIME SERIES OF CO_2 PERTURBATION SYMMETRIC?

The previous section discussed *time-average profiles* of $c(z,t)$, and particularly the cause of vertically uniform time-average profiles. This section discusses periodic time *series* of $c(z,t)$, and the cause of equal but opposite values of $c(z,t)$ during day and night, as would occur in our model for an unrectified solution.

We prove that if $c(z,t)$ is a solution of the diffusion equation (5) with boundary conditions (6) and (7), and if

$$K(z,t) = K(z,t+\pi) \qquad S(t) = -S(t+\pi), \quad (12)$$

then $-c(z,t+\pi)$ is also a solution. Here an eddy diffusivity $K(z,t) = K(z,t+\pi)$ means simply that K is periodic with a period of one-half day. In other words, K, and hence the transport, behaves the same during the day as during the night, as would be the case in an unrectified situation. The source $S(t)$ is assumed to have day-night anti-symmetry and zero diurnal mean. The proof simply involves letting $t \to t+\pi$ in Eqs. (5), (6), and (7). By inspection, one sees that $-c(z,t+\pi)$ satisfies the equation (5) and boundary conditions (6-7).

If both $c(z,t)$ and $-c(z,t+\pi)$ are solutions, then, because of linearity, there also exists the solution

$$c_a(z,t) = \frac{c(z,t) - c(z,t+\pi)}{2}, \quad (13)$$

which also satisfies the boundary conditions (6-7). If $c_a(z,t)$ has a period of 2π, then, it is straightforward to show, by integration of (13) over a period, that

$$\overline{c_a(z,t)}^t = 0. \quad (14)$$

That is, c_a has a profile that is uniform with height. Inspection of (13) reveals that $c_a(z,t)$ obeys the following periodic anti-symmetry:

$$c_a(z,t) = -c_a(z,t+\pi). \quad (15)$$

In such solutions, the perturbation mixing ratio at one time is the opposite of what it is a half-day earlier or later. For instance, a reduction of CO_2 during the day matches an equal but opposite increase in CO_2 during the night.

Perhaps of more interest is to demonstrate the converse, that is, that if $K(z,t) \neq K(z,t+\pi)$, then $c_a(z,t) = -c_a(z,t+\pi)$ cannot be a solution. In other words, if the transport differs between night and day, then the CO_2 time evolution must be asymmetric (e.g. rectified) and not, for instance, sinusoidal (unrectified). We defer the derivation to Larson and Volkmer (2008), who prove that this is true wherever and whenever $\partial c_a/\partial z$ is non-zero.

5. MODEL SOLUTIONS

5.1 A general, periodic, series solution

For the remainder of this paper, we will assume that the eddy diffusivity, K, is independent of altitude. Clearly this is a crude approximation for the earth's atmosphere. However, the assumption permits simple analytic solutions that are qualitatively realistic. We prescribe a sinusoidal diurnal cycle in K:

$$K = 1 - \alpha\cos(t). \quad (16)$$

Here, α is a parameter that lies within the range $0 \leq \alpha < 1$. Given the model (16), K is greater during the day, when the ground is heated and turbulent convection is more common, and lesser at night, when the atmosphere is often stably stratified. In this case, K does not have the day-night symmetry (12), and hence $c(z,t)$ is not expected to have equal but opposite values during the day as during night.

In the remainder of this section (Section 5), we will set the source $S(t) = 0$, for simplicity. We seek a time-periodic solution to the diffusion equation (5) with boundary conditions (6) and (7). We use separation of variables for z and t (e.g. Chapter 13 of Boas 1983). That is, we seek solutions of a special form in which the variables z and t appear in separate functions, which we denote Z and T. Since the equation for c is linear, such solutions may be summed:

$$c(z,t) = \sum_m Z_m(z)T_m(t). \quad (17)$$

After standard manipulations, we find the following series solution to (5):

$$c(z,t) = \sum_{m=1}^{\infty} \frac{A_m}{\sqrt{m}} e^{-\sqrt{m}z} \left[\cos\psi - \sin\psi\right], \quad (18)$$

where

$$\psi \equiv \sqrt{m}z - mt + m\alpha\sin(t). \quad (19)$$

We have retained only the solution that decays as $z \to \infty$ in order to satisfy the upper boundary condition (7).

We choose the A_m coefficients such that they satisfy the lower boundary condition (6) (see Larson and Volkmer (2008))

$$A_m = \frac{2}{\alpha} J_m(m\alpha). \quad (20)$$

Here J_m is the mth Bessel function.

The time-average concentration is:

$$\overline{c(z,t)}^t = \sum_{m=1}^{\infty} \frac{A_m}{\sqrt{m}} J_m(m\alpha) e^{-\sqrt{m}z} \left[\cos(\sqrt{m}z) - \sin(\sqrt{m}z)\right]. \quad (21)$$

By substituting (20) into (21), we see that at the surface $(z=0)$, (21) reduces to

$$\overline{c(z=0,t)}^t = \frac{2}{\alpha} \sum_{m=1}^{\infty} \frac{\left[J_m(m\alpha)\right]^2}{\sqrt{m}}. \quad (22)$$

By Taylor expanding the Bessel functions in polynomials about $\alpha = 0$ (Eq. 9.1.10 Abramowitz and Stegun 1965), we find the approximate form

$$\overline{c(z=0,t)}^t \approx 0.5\alpha + 0.229\alpha^3 + 0.143\alpha^5. \quad (23)$$

Recall that $c(z,t)$ is the non-dimensionalized, perturbation mixing ratio: $c(z,t) = (\tilde{c}(\tilde{z},\tilde{t}) - \tilde{c}_{\rm ref})/c_0$. In dimensional form, Eq. (23) becomes

$$\overline{\tilde{c}(\tilde{z}=0,\tilde{t})}^{\tilde{t}} \approx \tilde{c}_{\rm ref} + \frac{F_0}{\sqrt{2\omega_0 K_0}}\left(0.5\alpha + 0.229\alpha^3 + 0.143\alpha^5\right). \quad (24)$$

These formulas indicate how the rectifier parameter α affects the average surplus surface CO_2 mixing ratio associated with the rectifier effect.

5.2 A simple model with a closed-form asymmetric solution

If we desire to find an exact solution that has only one term, then we may modify the lower boundary condition as follows:

$$-\frac{K}{2}\frac{\partial c}{\partial z}\bigg|_{z=0} = [1-\alpha\cos(t)]\cos[t-\alpha\sin(t)]. \quad (25)$$

This boundary condition is more complex and less realistic than the boundary condition (6), but it leads to a simple solution. (Since this boundary condition does not have the symmetry of $\cos(t)$ in general, it does not permit the symmetry arguments of the previous section.) Again using separation of variables, we find

$$c(z,t) = e^{-z}\left\{\cos[z-t+\alpha\sin(t)] - \sin[z-t+\alpha\sin(t)]\right\}. \quad (26)$$

One can time-average this solution over a diurnal cycle to find an averaged CO_2 mixing ratio, $\overline{c(z,t)}^t$. One finds

$$\overline{c(z,t)}^t = J_1(\alpha)e^{-z}[\cos(z) - \sin(z)]. \quad (27)$$

For small α (Eq. 9.1.10 Abramowitz and Stegun 1965),

$$J_1(\alpha) \approx \frac{1}{2}\alpha. \quad (28)$$

5.3 A special case: An anti-symmetric solution

The previous solutions permit $\alpha \neq 0$, in which case K does not obey the day-night symmetry (12), and hence $\overline{c(z,t)}^t \neq 0$. In contrast, when $\alpha = 0$, then $K = 1$ and $c(z,t)$ becomes anti-symmetric with $\overline{c(z,t)}^t = 0$.

Here, for purposes of comparison with the previous solutions, we set $\alpha = 0$ and $K = 1$ in the governing equation (5) and boundary conditions (6) and (7). We find, e.g. via separation of variables, that a time-periodic solution is

$$c(z,t) = e^{-z}[\cos(z-t) - \sin(z-t)]. \quad (29)$$

This is also the solution to which (27) reduces when $\alpha = 0$. Because K has the symmetry (12), the solution has the anti-symmetry of $c_a(z,t)$ (15), as expected by our symmetry proof of Section 4. Furthermore, the diurnal average is

$$\overline{c(z,t)}^t = 0, \quad (30)$$

as expected by our proof of Section 3. The solution is un-rectified.

5.4 Plots of solutions

By varying the rectifier parameter α, the series solution (18) allows us to compute solutions that range from perfectly symmetric and unrectified ($\alpha = 0$) to highly asymmetric and rectified (e.g. $\alpha = 0.95$). These two extremes are plotted, respectively, in the left and right columns of Figure 1.

The top right-hand panel (rectified case) shows a sharp peak of CO_2 mixing ratio at night and a deeper layer during the day. The diurnal-mean profile of CO_2 in the top right panel is rectified and looks qualitatively similar to the observations presented in Figure 3(a) of Yi et al. (2004).

The middle row plots the eddy diffusivity, the surface CO_2 mixing ratio, and the surface CO_2 flux. The surface mixing ratio is symmetric with time in the unrectified case (middle left panel) and asymmetric in the rectified case (middle right panel) as expected from the symmetry proof of Section 4. The surface CO_2 flux in either case is prescribed to be a cosine and appears qualitatively similar to observations shown in Figure 3 of Davis et al. (2003) and Figure 7 of Baker et al. (2003).

The bottom row shows the time series of CO_2 mixing ratio at various altitudes. The unrectified solutions are symmetric with time, as expected. The rectified solutions have features that agree qualitatively with the observations in Yi et al. (2000). For instance, mixing ratios vary strongly with altitude at night, when the boundary layer is stratified, and the mixing ratios vary little with altitude during the day, when the boundary layer is better mixed (see, e.g., Figure 10 of Chen et al. (2004)).

6. INVERSE MODELING

The dimensionless model described above quantifies the strength of the rectifier effect in terms of a single dimensionless parameter, α. The simplicity of the model facilitates inverse modeling. In a typical CO_2 inverse model calculation, one measures the CO_2 mixing ratio in the atmosphere and infers the net flux of CO_2 into the atmosphere from the underlying land or ocean surface. The surface flux provides information about sources and sinks of CO_2 such as growth of biomass via photosynthesis. An advantage of using CO_2 mixing ratio to infer CO_2 flux is that it provides an estimate of the flux over a broader region than is possible using a single direct measurement of CO_2 flux.

To illustrate how the above model of the rectifier effect can simplify inverse calculations, we consider the 1D problem of separately inferring the daytime and

nighttime surface CO_2 fluxes. This might be useful because it begins to help separate the sink of CO_2 due to daytime photosynthesis from sources such as nighttime respiration.

As input data for our problem, suppose that we measure a continuous time series of CO_2 concentration measurements at the ground and at one higher altitude. Such measurements are taken at several research towers across the globe (Bakwin et al. 2004). The output of our inverse calculation is a complete but approximate solution of 1D (vertical) CO_2 evolution and transport, including the amplitude of the diurnally varying flux, F_0 of Eq. (2).

For simplicity, we assume that the internal atmospheric "source" of CO_2, $\tilde{S}$, is known. This "source" could crudely represent horizontal advection of CO_2 into or out of the 1D grid column of interest. The four input measurements are: the first and second Fourier cosine coefficients $\tilde{a}_1$ and $\tilde{a}_2$ of the CO_2 time series, and the mean at the surface, $\overline{\tilde{c}(\tilde{z}=0,\tilde{t})}^{\tilde{t}}$ and at some altitude aloft, $\overline{\tilde{c}(\tilde{z}=\tilde{z}_1,\tilde{t})}^{\tilde{t}}$. The four unknown parameters of the problem and the equations that define them are α (16), c_0 (4), F_0 (2), and $\tilde{c}_{\mathrm{ref}}$ (8).

The inversion procedure involves four straightforward steps that we will not discuss here but instead defer to Larson and Volkmer (2008). We merely note that our analytic forward model simplifies the inverse calculation because the strength of the rectifier in this simplified model depends only on a single parameter, α, and therefore the inverse calculation requires that we numerical calculate only two single-variable roots. Finding such single-variable roots typically requires little computational time.

7. CONCLUSIONS

We have constructed an idealized model of the vertical CO_2 rectifier effect. In the model, transport of CO_2 is represented by a prescribed eddy diffusivity. The key feature of the model is that the eddy diffusivity varies diurnally. During the day, the eddy diffusivity is larger, representing daytime convective vertical transport; during the night, the eddy diffusivity is smaller, representing nighttime stable stratification and weak vertical transport.

Prior authors have noted that the diurnal rectifier effect arises from non-zero covariance of CO_2 surface flux and CO_2 vertical transport (e.g. Denning et al. 1996b). We prove a somewhat similar relationship in Section 3. Specifically, we show that in our model, the time-averaged profile of CO_2 mixing ratio is uniform in the vertical (as typical for an unrectified solution) if and only if there is zero covariance in time between the perturbation eddy diffusivity and vertical gradient of CO_2 mixing ratio. Relatedly, we also show that the existence of the rectifier effect in our model depends on whether the vertical transport behaves the same during day as during night (see Section 4). Specifically, we prove that the diurnal cycle of CO_2 mixing ratio in our model is asymmetric (as typical for a rectified case) if and only if the eddy diffusivity is not [periodic with a period of one-half day]. This proof relies on the fact that our model's CO_2 surface flux has day-night anti-symmetry.

The point of these proofs is isolate the essential ingredients needed in an eddy diffusivity model to yield a rectified or unrectified profile.

Our rectifier model can be solved analytically in terms of an infinite series solution (18). In nondimensionalized form, the model equations and solutions depend on a single parameter, α. This rectifier parameter represents the degree of day-night difference in the magnitude of eddy diffusivity (see Eq. 16). When $\alpha = 0$, the eddy diffusivity is constant and the rectifier effect vanishes. When α approaches 1, the eddy diffusivity is much stronger during the day than at night, and the rectifier effect is pronounced.

The rectifier parameter α can be simply but quantitatively related to the surplus surface CO_2 mixing ratio associated with the rectifier effect. We find a relationship in the form of an exact infinite series (22) and a Taylor series approximation valid for small α (23). In this way, the single parameter that represents diurnal variations in turbulent transport, namely α, can be directly linked to the strength of the rectifier effect.

Because the single-parameter solution (18) is simple, it facilitates inverse computations. As an example, Larson and Volkmer (2008) discuss the construction of a complete, 1D, time-evolving solution for CO_2, given a measurement of the time series of CO_2 mixing ratio at a location at the surface and at a single higher altitude. The solution includes the amplitude of the diurnal surface flux of CO_2.

In addition to facilitating inverse computations, the model illustrates conceptual points that may apply to more sophisticated inverse methods (see Larson and Volkmer 2008). For instance, the equations reveal that this particular diurnal rectifier inversion problem has some potential pitfalls. Specifically, inferring the depth of vertical transport requires measurement at two or more altitudes. Therefore, a surface measurement alone is insufficient if vertical transport is unknown — additional measurements are required, from a tower for instance. This is because surface CO_2 time series are fundamentally ambiguous in this 1D setting: the same time series may arise from strong surface flux and transport, or weak flux and transport. Furthermore, when CO_2 is measured at two and only two altitudes, there may remain further ambiguities. If the measurement altitude aloft is too low, the inverse estimate may be imprecise when CO_2 mixing is deep. When the altitude of measurement is about the same as the depth over which CO_2 mixes, then the solution may be non-unique. We speculate that measurements at multiple, strategically chosen altitudes would resolve these problems. The above considerations may prove useful in design of field measurements of CO_2 mixing ratio.

In a future application, the prescribed diurnal eddy diffusivity (16) and surface flux (6) could be imposed for

CO_2 in each grid column of an atmospheric model with three spatial dimensions. The strength of the rectifier effect could then be specified by setting the parameter α. By performing sensitivity studies with different values of α, one could explore how the rectifier effect combines with three-dimensional transport to produce large-scale patterns of CO_2 mixing ratio. If the mixing ratio of CO_2 at a particular surface point in the atmospheric model differs from the value expected by 1D theory (i.e., Eq. 18), then it indicates that 3D transport has a significant effect at that point.

8. ACKNOWLEDGMENTS

V. E. Larson is grateful for financial support from a Research Growth Initiative Award from the University of Wisconsin — Milwaukee.

References

Abramowitz, M. and I. A. Stegun, 1965: *Handbook of mathematical functions*. Dover Publications, 1046 pp.

Baker, I., A. S. Denning, N. Hanan, L. Prihodko, M. Uliasz, P.-L. Luigi, K. Davis, and P. Bakwin, 2003: Simulated and observed fluxes of sensible and latent heat and CO_2 at the WLEF-TV tower using SiB2.5. *Global Change Biology*, **9**, 1262–1277.

Bakwin, P. S., K. J. Davis, C. Yi, S. C. Wofsy, J. W. Munger, L. Haszpra, and Z. Barcza, 2004: Regional carbon dioxide fluxes from mixing ratio data. *Tellus*, **56B**, 301–311.

Boas, M. L., 1983: *Mathematical Methods in the Physical Sciences*. 2nd edition, John Wiley and Sons, 793 pp.

Braswell, B. H., W. J. Sacks, E. Linder, and D. S. Schimel, 2005: Estimating diurnal to annual ecosystem parameters by synthesis of a carbon flux model with eddy covariance net ecosystem exchange observations. *Global Change Biology*, **11**, 335–355.

Chen, B., J. M. Chen, J. Liu, D. Chan, K. Higuchi, and A. Shashkov, 2004: A vertical diffusion scheme to estimate the atmospheric rectifier effect. *J. Geophys. Res.*, **109**. Doi:10.1029/2003JD003925.

Davis, K. J., P. S. Bakwin, C. Yi, B. W. Berger, C. Zhao, R. M. Teclaw, and J. G. Isebrands, 2003: The annual cycles of CO_2 and H_2O exchange over a northern mixed forest as observed from a very tall tower. *Global Change Biology*, **9**, 1278–1293.

Denning, A. S., I. Y. Fung, and D. A. Randall, 1995: Latitudinal gradient of atmospheric CO_2 due to seasonal exchange with land biota. *Nature*, **376**, 240–243.

Denning, A. S., G. J. Collatz, C. Zhang, D. A. Randall, J. A. Berry, P. J. Sellers, G. D. Colello, and D. A. Dazlich, 1996a: Simulations of terrestrial carbon metabolism and atmospheric CO_2 in a general circulation model. Part 1: Surface carbon fluxes. *Tellus*, **48B**, 521–542.

Denning, A. S., D. A. Randall, G. J. Collatz, and P. J. Sellers, 1996b: Simulations of terrestrial carbon metabolism and atmospheric CO_2 in a general circulation model. Part 2: Simulated CO_2 concentrations. *Tellus*, **48B**, 521–542.

Denning, A. S., T. Takahashi, and P. Friedlingstein, 1999: Can a strong atmospheric CO_2 rectifier effect be reconciled with a "reasonable" carbon budget? *Tellus*, **51B**, 249–253.

Gurney, K. R., R. M. Law, A. S. Denning, P. J. Rayner, D. Baker, P. Bousquet, L. Bruhwiler, Y.-H. Chen, P. Ciais, S. Fan, I. Y. Fung, M. Gloor, M. Heimann, K. Higuchi, J. John, T. Maki, S. Maksyutov, K. Masarie, P. Peylin, M. Prather, B. C. Pak, J. Randerson, J. Sarmiento, S. Taguchi, T. Takahashi, and C.-W. Yuen, 2002: Towards robust regional estimates of CO_2 sources and sinks using atmospheric transport models. *Nature*, **415**, 626–630.

Gurney, K. R., R. M. Law, A. S. Denning, P. J. Rayner, D. Baker, P. Bousquet, L. Bruhwiler, Y.-H. Chen, P. Ciais, S. Fan, I. Y. Fung, M. Gloor, M. Heimann, K. Higuchi, J. John, E. Kowalczyk, T. Maki, S. Maksyutov, P. Peylin, M. Prather, B. C. Pak, J. Sarmiento, S. Taguchi, T. Takahashi, and C.-W. Yuen, 2003: TransCom 3 CO_2 inversion intercomparison: 1. Annual mean control results and sensitivity to transport and prior flux information. *Tellus*, **55B**, 555–579.

Heimann, M., C. D. Keeling, and I. Y. Fung, 1986: Simulating the atmospheric carbon dioxide distribution with a three-dimensional tracer model. *The changing carbon cycle: A global analysis*, J. R. Trabalka and D. E. Reichle, Eds., Springer-Verlag, 16–49.

Keeling, C. D., S. C. Piper, and M. Heimann, 1989: A three-dimensional model of atmospheric CO_2 transport based on observed winds: 4. Mean annual gradients and interannual variations. *Aspects of climate variability in the Pacific and the Western Americas*, D. H. Peterson, Ed., Geophys. Monogr. 55, Am. Geophys. Union, 305–363.

Larson, V. E. and H. Volkmer, 2008: An idealized model of the one-dimensional carbon dioxide rectifier effect. *Tellus*, **60B**, 525–536.

Law, R. M., P. J. Rayner, and Y. P. Wang, 2004: Inversion of diurnally varying synthetic CO_2: Network optimization for an Australian test case. *Global Biogeochemical Cycles*, **18**, GB1044. Doi:10.1029/2003GB002136.

Peylin, P., P. J. Rayner, P. Bousquet, C. Carouge, F. Hourdin, P. Heinrich, and P. Ciasis, 2005: Daily CO_2 flux estimates over Europe from continuous atmospheric measurements: 1, inverse methodology. *Atmos. Chem. Phys. Discuss.*, **5**, 1647–1678.

Stephens, B. B., S. C. Wofsy, R. F. Keeling, P. P. Tans, and M. J. Potosnak, 2000: The CO_2 budget and rectification airborne study: Strategies for measuring rectifiers and regional fluxes. *Inverse Methods in Global Biogeochemical Cycles*, P. K. et al., Ed., volume 114 of *Geophys. Monogr. Ser.*, American Geophysical Union, Washington, D.C., 311–324.

Stephens, B. B., K. R. Gurney, P. P. Tans, C. Sweeney, W. Peters, L. Bruhwiler, P. Ciais, M. Ramonet, P. Bousquet, T. Nakazawa, S. Aoki, T. Machida, G. Inoue, N. Vinnichenko, J. Lloyd, A. Jordan, M. Heimann, O. Shibistova, R. L. Langenfelds, L. P. Steele, R. J. Francey, and A. S. Denning, 2007: Weak northern and strong tropical land carbon uptake from vertical profiles of atmospheric CO_2. *Science*, **316**, 1732–1735.

Stull, R. B., 1988: *An Introduction to Boundary Layer Meteorology*. Kluwer Academic Publishers, 666 pp.

Yi, C., K. J. Davis, P. S. Bakwin, B. W. Berger, and L. C. Marr, 2000: Influence of advection on measurements of the net ecosystem-atmosphere exchange of CO_2 from a very tall tower. *J. Geophys. Res.*, **105**, 9991–9999.

Yi, C., K. J. Davis, B. W. Berger, and P. S. Bakwin, 2001: Long-term observations of the dynamics of the continental planetary boundary layer. *J. Atmos. Sci.*, **58**, 1288–1299.

Yi, C., K. J. Davis, P. S. Bakwin, A. S. Denning, N. Zhang, A. Desai, J. C. Lin, and C. Gerbig, 2004: Oberved covariance between ecosystem carbon exchange and atmospheric boundary layer dynamics at a site in northern Wisconsin. *J. Geophys. Res.*, **109**. Doi:10.1029/2003JD004164.

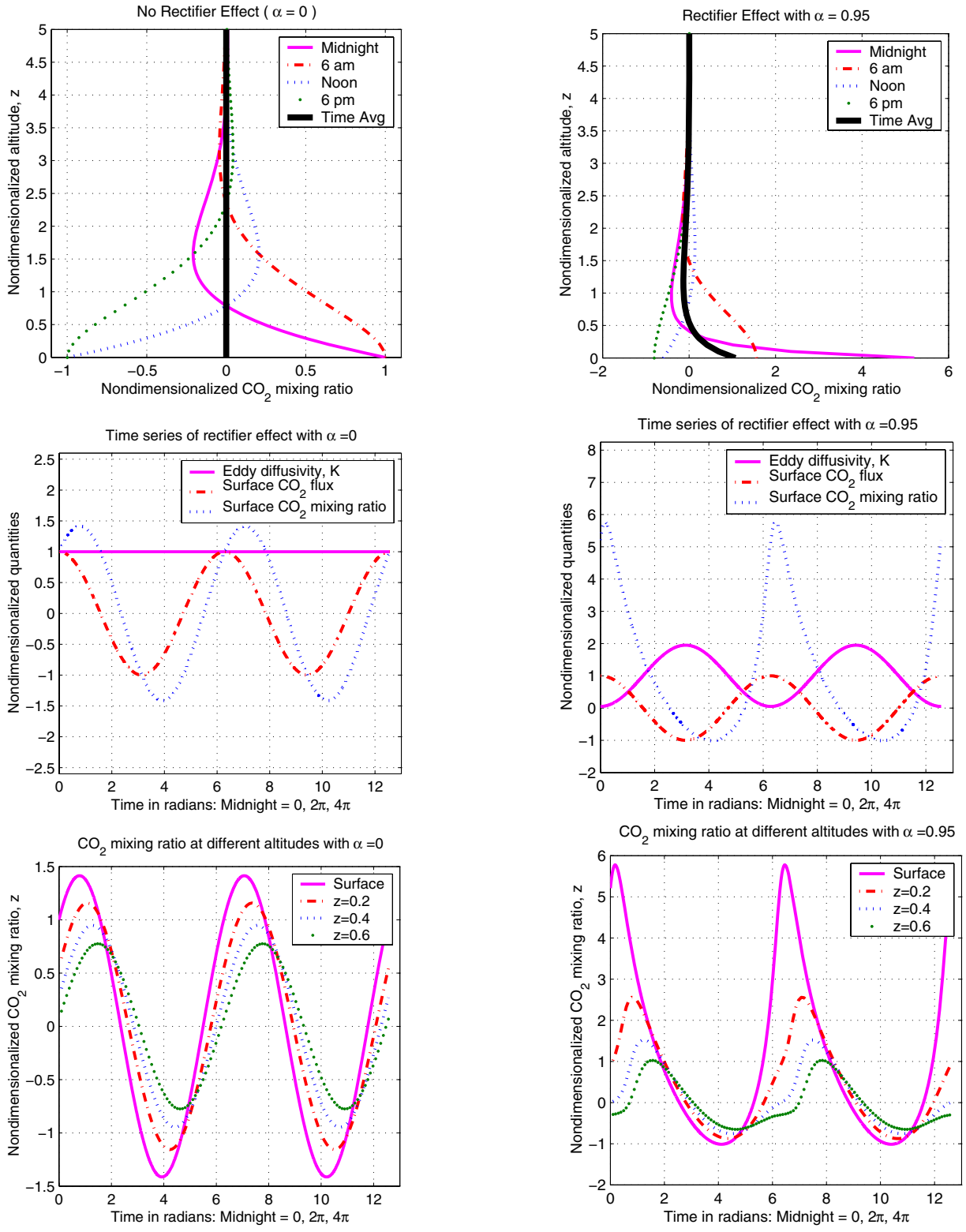

Figure 1: Plots of the model solution for CO_2 mixing ratio (Eq. 18), eddy diffusivity (Eq. 16), and CO_2 flux at the surface (Eq. 6). The left column of panels has no rectification ($\alpha = 0$), and the right column of panels has strong rectification ($\alpha = 0.95$). The top right-hand panel shows that the time-averaged rectified profile of CO_2 mixing ratio has an excess of CO_2 near the surface and a deficit aloft. The middle row shows that the time series of surface CO_2 mixing ratio when $\alpha = 0.95$ has a classic rectified shape (middle right panel), with a sharp peak at night and a moderate minimum during the day; when $\alpha = 0$ (middle left panel), the time series is sinusoidal. The bottom row of panels shows that with $\alpha = 0.95$, the CO_2 mixing ratio is stratified at night but more well-mixed during the day.